PERGAMON

International Journal of Heat and Mass Transfer 44 (2001) 2583–2587

International Journal of HEAT and MASS TRANSFER

www.elsevier.com/locate/ijhmt

Technical Note

Effect of circumferential variation of sidewall temperature on buoyant convection in a vertical cylinder

Kwang Hyo Chung, Jae Min Hyun *

Department of Mechanical Engineering, Korea Advanced Institute of Science and Technology, 373-1 Kusong-dong, Yusung-gu, Taejon 305-701, South Korea

Received 25 February 2000; received in revised form 7 July 2000

1. Introduction

Recently, notable progress has been made in numerical computations of three-dimensional features of buoyant convection in an enclosure [1–6]. As in technological applications, interest is confined to the situations in which the representative Rayleigh number is large. The overall flow pattern is of boundary layer-type; the global flow can be divided into boundary layers adjacent to the solid walls, and interior core.

By resorting to a systematic analytical approach, Jischke and Doty [7] presented a theoretical description of flow in an arbitrarily shaped container on which a gravitationally-stable vertical temperature distribution was imposed. One important dynamical element is the horizontal nonuniformities of boundary temperature. Examples may readily be seen in a fuel tank exposed to oblique insolation. The effect of continuous variation of the boundary temperature along the circumference on the buoyant convection inside the container warrants an in-depth scrutiny. As a straightforward illustration of the exposition of [7], Chung et al. [8] carried out full-dress numerical calculations to depict the three-dimensional flow and temperature fields in a vertically mounted cylinder. In [8], the temperature at the cylindrical sidewall T_w was vertically uniform but it had a sinusoidal variation in the azimuthal direction, $T_w = T_m[1 + (1/2)\cos(n\phi)]$, n being an integer, where ϕ denotes the azimuthal angle (in radian). The temperature T_h at the hot spots, $\phi = 2\pi/n$, is $T_h = 1.5T_m$ and the temperature T_c at the cold spots, $\phi = \pi/n$, is $T_c = 0.5T_m$. In this model, the value of ΔT $[\equiv T_h - T_c] = T_m$ is altered to produce the desired value of Ra. Obviously, for a given n, the wavelength of the sidewall temperature variation is $1/n$ of the circumference of the cylinder. Computed results for the rudimentary case $n = 1$ were displayed in [8]. These demonstrated that the direct effect of the azimuthal variation of T_w is substantially absorbed in the boundary layer and the interior core is largely horizontally uniform and stably-stratified.

As a sequel to [8], this note intends to delineate the global flow features when the severity of azimuthal variation of T_w is intensified. The intention here is to probe into the changes in flow character as n is increased, i.e., the azimuthal gradient of T_w increases.

2. Model

An incompressible Boussinesq-fluid is contained in a vertical cylinder [radius R_c, height H], as sketched in Fig. 1. The Rayleigh number Ra $[\equiv g\beta(T_h - T_c)H^3/\nu\alpha]$, in which g denotes gravity, β coefficient of thermometric expansion, ν kinematic viscosity and α thermal diffusivity, is set $Ra = 10^6$, the Prandtl number Pr $[\equiv \nu/\alpha] = 0.71$, and the cylinder aspect ratio A_r $[\equiv H/R_c] = 2.0$. The nondimensional governing Navier–Stokes equations and the numerical computational procedures were elaborated in [8].

3. Results and discussion

3.1. Flow and temperature fields

Fig. 2 displays the isotherms $[\theta \equiv (T - T_m)/(T_h - T_c)]$ and nondimensional velocity vectors $[(U, V, W) \equiv (uR_c/$

* Corresponding author. Tel.: +82-42-869-3012; fax: +82-42-869-3210.

E-mail address: jmhyun@cais.kaist.ac.kr (J.M. Hyun).

PII: S0017-9310(00)00277-5

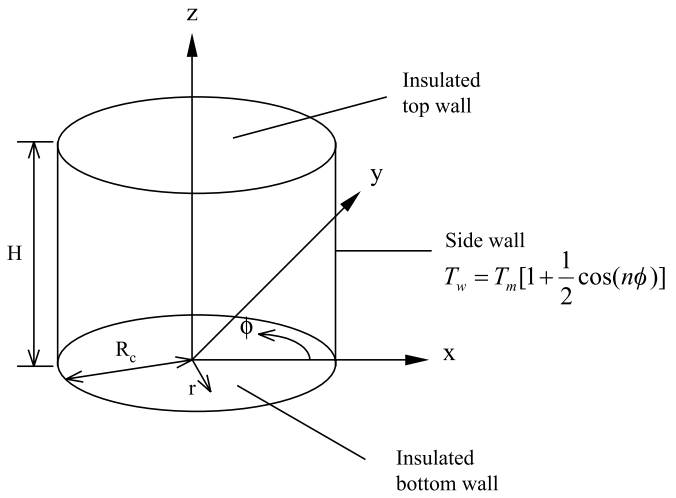

Fig. 1. Flow configuration and coordinates.

$\alpha, vR_c/\alpha, wR_c/\alpha)]$ in the meridional plane at $\phi = 0$, the principal plane containing T_h; $\phi = \pi/2n$, the neutral plane containing T_m $[= (T_h + T_c)/2]$; $\phi = \pi/n$, the principal plane containing T_c. For all the cases computed, the interior core is substantially stably stratified. The velocity vectors in the principal meridional planes in the interior core are generally small in magnitude, and the flow is concentrated to the boundary layers. It is also noted that, for all n, in the principal planes, the flow in the vertical boundary layer is in one direction, i.e., upward for the plane of T_h and downward for the plane of T_c. In the neutral plane, the interior flow is seen to be appreciable in strength, and this trend is more conspicuous for smaller n. However, in the neutral plane, the overall flow diminishes for large n. The flows in the vertical boundary layer are directed toward the mid-height. After meeting near the mid-height, the flow turns radially inward horizontally.

As n increases, in the principal planes, the horizontal boundary-layer flows weaken, and these flows cannot penetrate to the axis of the cylinder. The isotherms in the axis area become highly flat and less strongly stratified, which reveals an appreciable influence of conduction in this localized region. A similar trend is discernible in the neutral plane. In summary, for larger n, the flow weakens in general and is further concentrated to the vertical boundary layer, and the stratification in the interior is lessened.

The vertical temperature distribution in the mid-height region $[Z(\equiv z/R_c) \cong 0.5 \sim 1.5]$ at the axis does not change much as n varies. However, the temperature variations near the horizontal walls are more steep for smaller n.

The flow behavior on the horizontal planes is exemplified in Fig. 3. In the bulk of the interior away from the mid-height, $2n$ circulating cells of horizontal flows are visible. In the mid-height region, due to the symmetry condition, the horizontal flows constitute $4n$ cells. In the temperature field, it is clear that the azimuthal variations of wall temperature are largely absorbed in the boundary layer. Consequently, the interior core is substantially in uniform temperature [8]. The weakening of horizontal flows in the mid-height zones is also apparent. The concentration of vertical flows in the vertical boundary layer is manifested. As stressed earlier, as n increases, the horizontal flows are reduced in magnitude and the majority of the interior is nearly stagnant for large n.

3.2. Heat transfer on the cylindrical surface

On the cylindrical surface $[R(\equiv r/R_c) = 1]$, the local Nusselt number Nu is defined as

$$Nu = \left.\frac{\partial\theta}{\partial R}\right|_{R=1}. \tag{1}$$

The Nu patterns are illustrated in Figs. 4(a)–(c) over a wavelength of azimuthal angle, i.e., $\phi = 0$ to $\phi = 2\pi/n$. The maximum/minimum value of Nu is seen to be located in the lower/upper region of the hot $(T_w = T_h)$/cold $(T_w = T_c)$ portion of the wall. These regions correspond to vigorous rising/sinking motions in the vertical boundary layer. Furthermore, the spatial gradients of Nu are pronounced in these areas. On the contrary, in the mid-height zones, spatial variations in Nu weaken. It is also noted that, as n increases, the maximum value of Nu is slightly lowered. This again reflects the fact that, for larger n, the overall strength of flow in the boundary layer is reduced.

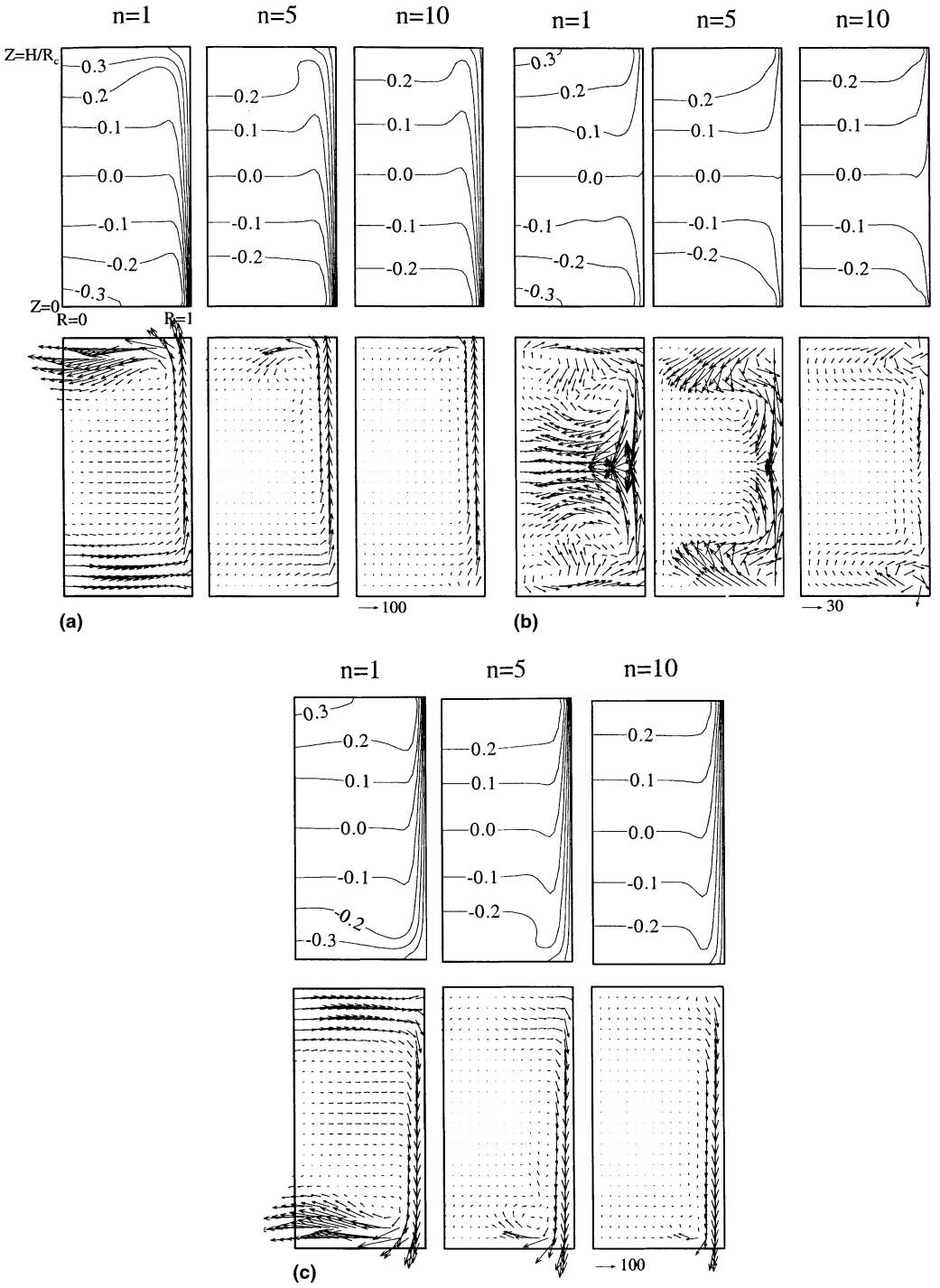

Fig. 2. Temperature (upper row) and velocity (lower row) fields on the meridional planes: (a) principal meridional plane of $\phi = 0$ ($T_w = T_h$); (b) neutral meridional plane for $T_w = T_m$; (c) principal meridional plane for $T_w = T_c$.

It is useful to define the gain factor G, which denotes the heat transport by convection relative to conduction, $G \equiv q''_{conv}/q''_{cond}$. The conductive mean heat flux, q''_{cond}, from hot sectors (in which $\theta > 0$) can be computed by utilizing the conduction solution for this geometry, $\theta = 0.5R^n \cos(n\phi)$:

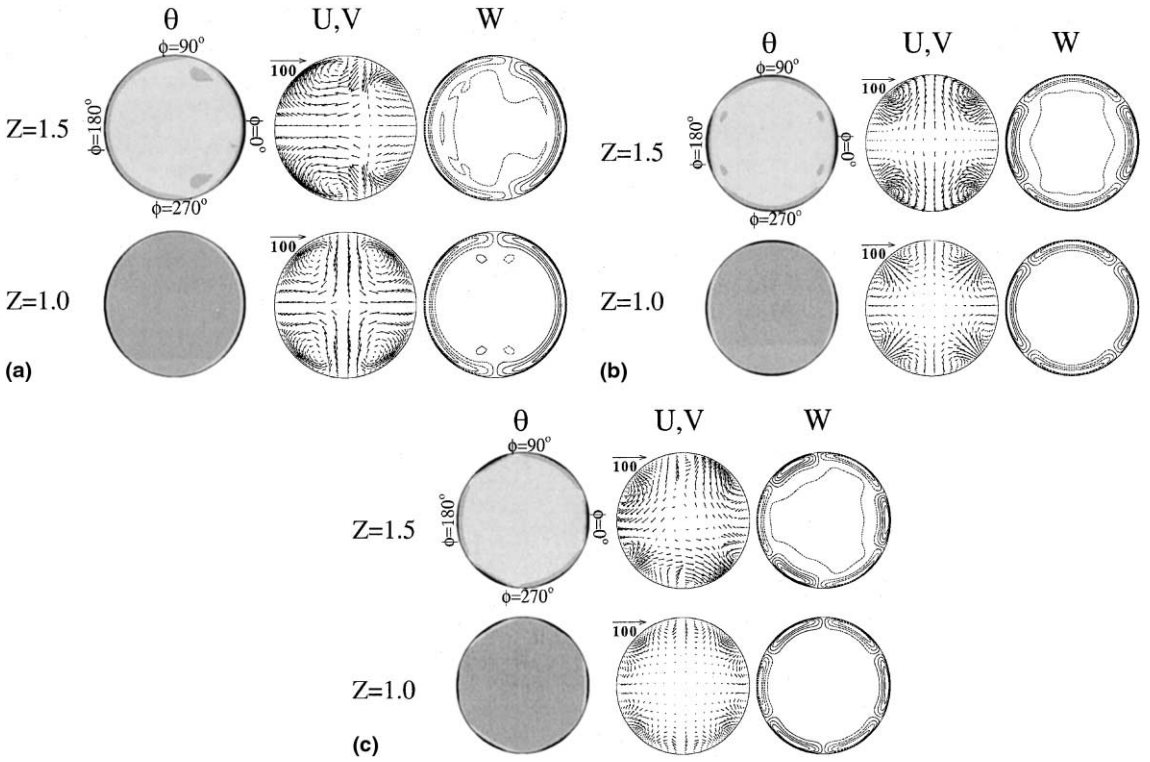

Fig. 3. Temperture (θ) and velocity fields on planes of constant height. U,V denote the horizontal velocities, and W denote the vertical velocity. (a) $n=1$, (b) $n=2$, (c) $n=3$.

$$q''_{\mathrm{cond}} = \left(2n \int_0^H \int_0^{\pi/2n} k \left. \frac{\partial T}{\partial r} \right|_{r=R_c} R_c \, \mathrm{d}\phi \, \mathrm{d}z \right) \Big/ (\pi R_c H)$$

$$= \frac{kn(T_h - T_c)}{\pi R_c}. \tag{2}$$

In the above, the relationship between the dimensional [T] and nondimensional [θ] temperature should be taken into account.

Similarly, the convective mean heat flux, q''_{conv}, can be computed:

$$q''_{\mathrm{conv}} = \left(2n \int_0^H \int_0^{\pi/2n} k \left. \frac{\partial T}{\partial r} \right|_{r=R_c} R_c \, \mathrm{d}\phi \, \mathrm{d}z \right) \Big/ (\pi R_c H)$$

$$= \frac{2kn(T_h - T_c)}{\pi H} \int_0^{H/R_c} \int_0^{\pi/2n} \left. \frac{\partial \theta}{\partial R} \right|_{R=1} \mathrm{d}\phi \, \mathrm{d}Z, \tag{3}$$

in which θ denotes the present numerical solution for temperature.

Therefore, the gain factor G is

$$G = \frac{2}{A_r} \int_0^{H/R_c} \int_0^{\pi/2n} \left. \frac{\partial \theta}{\partial R} \right|_{R=1} \mathrm{d}\phi \, \mathrm{d}Z. \tag{4}$$

Fig. 4(d) displays G versus n. As remarked previously, as n becomes large, the interior core, with very small velocities, occupies a wider area. Convective activities are less vigorous, which turns up in substantially reduced values of G.

4. Conclusion

As the azimuthal gradient of T_w is intensified (n increases), the flow in the interior weakens. The convective gain in heat transfer activities is reduced as n increases.

Acknowledgements

The authors are grateful to the referees for constructive comments. This work was supported by the

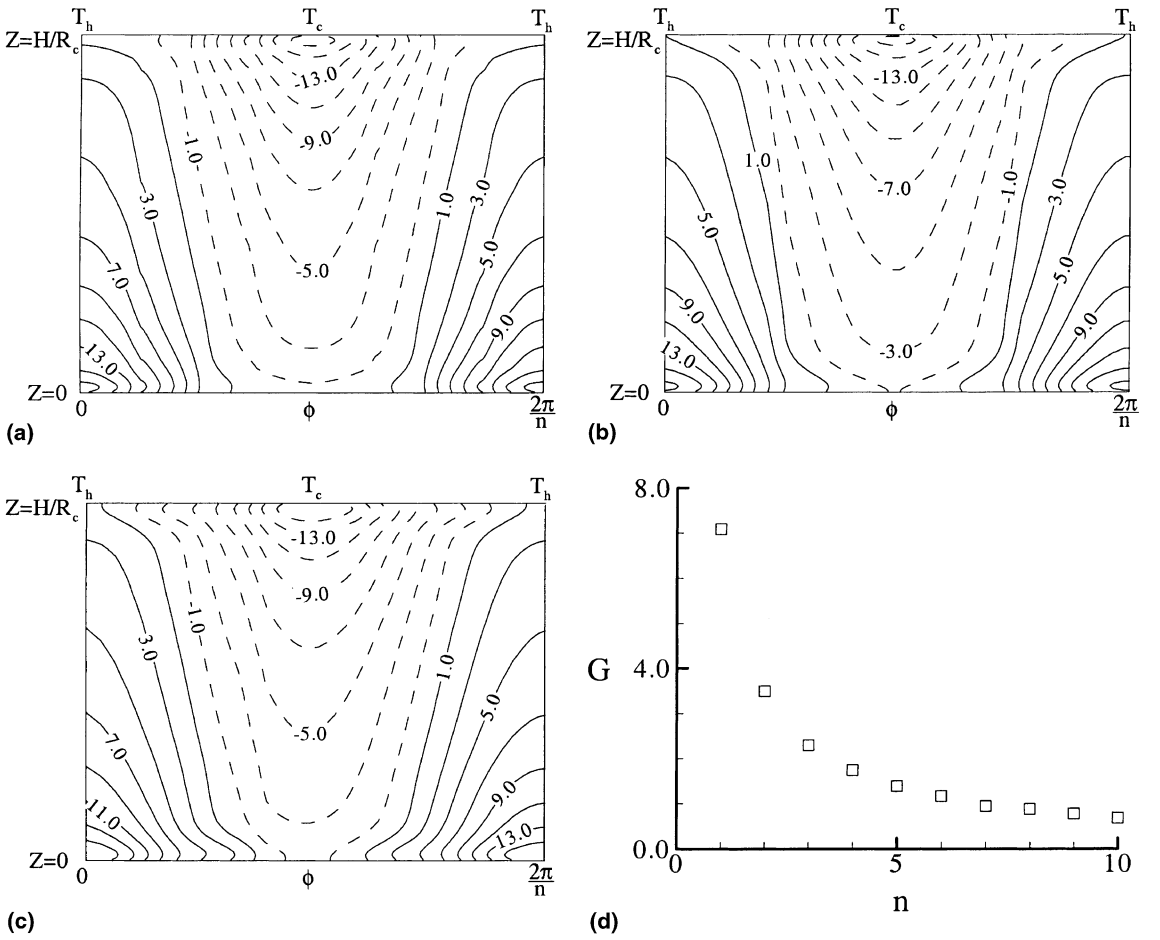

Fig. 4. Local Nusselt number *Nu* on the cylindrical surface and gain factor *G* in Eq. (4). (a) *Nu* for $n=1$, (b) *Nu* for $n=2$, (c) *Nu* for $n=3$, (d) *G*.

NRL Project (MOST), R & D Management Center for Energy and Resources, South Korea.

References

[1] T. Fusegi, J.M. Hyun, K. Kuwahara, B. Farouk, A numerical study of three-dimensional natural convection in a differentially heated cubical enclosure, Int. J. Heat Mass Transfer 34 (6) (1991) 1543–1557.

[2] C. Kleinstreuer, M. Lei, Transient buoyancy-induced three-dimensional flows in slender enclosures with coaxial heated cylinder, Int. J. Eng. Sci. 32 (10) (1994) 1635–1646.

[3] J.P. Pulicani, S. Krukowski, J. Iwan, D. Alexander, J. Ouazzani, F. Rosenberger, Convection in an asymmetrically heated cylinder, Int. J. Heat Mass Transfer 35 (9) (1992) 2119–2130.

[4] H. Potts, W.R. Wilcox, Thermal fields in the Bridgman–Stockbarger technique, J. Cryst. Growth 73 (1985) 350–358.

[5] E. Crespo, D. Arco, P. Bontoux, Numerical solution and analysis of asymmetric convection in a vertical cylinder: an effect of Prandtl number, Phys. Fluids A1 (8) (1989) 1348–1359.

[6] Y.H. Li, K.C. Lin, T.F. Lin, Computation of unstable liquid metal convection in a vertical closed cylinder heated from the side and cooled from above, Numerical Heat Transfer Part A 32 (1997) 289–309.

[7] M.C. Jischke, R.T. Doty, Linearized buoyant motion in a closed container, J. Fluid Mech. 71 (4) (1975) 729–754.

[8] K.H. Chung, J.M. Hyun, H. Ozoe, Buoyant convection in a vertical cylinder with azimuthally-varying sidewall temperature, Int. J. Heat Mass Transfer 43 (13) (2000) 2289–2301.